Dyes and Pigments 89 (2011) 97–104

Contents lists available at ScienceDirect

Dyes and Pigments

journal homepage: www.elsevier.com/locate/dyepig

Covalent attachment of 4-amino-1,8-naphthalimides onto the walls of mesoporous molecular sieves MCM-41 and SBA-15

Fabiane de Jesus Trindade, José Fernando Queiruga Rey, Sergio Brochsztain*

Petroleum Nanotechnology Group, Universidade Federal do ABC, Rua Santa Adélia, 166, Santo André-SP, 09210-170, Brazil

ARTICLE INFO

Article history:
Received 10 July 2010
Received in revised form
17 September 2010
Accepted 18 September 2010
Available online 29 September 2010

Keywords:
4-Amino-1,8-naphthalimides
Solid state fluorescence
Mesoporous materials
MCM-41
SBA-15
Inclusion complexes

ABSTRACT

This work describes the covalent grafting of 4-amino-1,8-naphthalimides, which are fluorescent dyes with very interesting optical properties, onto the walls of mesoporous molecular sieves. The mesoporous materials MCM-41 and SBA-15 were first treated with 3-aminopropyltriethoxysilane, generating amine-rich surfaces that were further reacted with 4-amino-1,8-naphthalic anhydride, resulting in yellow fluorescent solids. The success of the modification reactions was confirmed by elemental analysis, X-ray diffraction patterns, infrared spectroscopy, scanning electron microscopy and UV/visible and fluorescence spectroscopy. The emission spectra of the dye bound to MCM-41 was quite insensitive to solvent polarity, in contrast to dye-grafted SBA-15, which showed a high solvent sensitivity. These results suggest a tight fit of the dye molecules within the channels of MCM-41, leaving no room for the solvent molecules. In the case of SBA-15, the large pore size allows the invasion of the channels by solvent molecules, resulting in solvation of the encaged chromophore.

1. Introduction

Mesoporous molecular sieves are nanostructured materials obtained by surfactant-templated synthesis, resulting in highly ordered hexagonal arrays of one-dimensional, three-dimensional or wormlike channels, with large surface area and narrow pore size distribution [1,2]. Among the most well-known mesoporous molecular sieves are the MCM-41 [1] and SBA-15 [2] families, with pore sizes in the range 2–10 nm and 5–30 nm, respectively. Initially, researchers were interested in these materials as catalysts for the petroleum industry [3,4], in substitution for the zeolites. More recently, however, with the development of nanotechnology, it was acknowledged that these nanostructured materials have a great potential for novel applications in photonics and electronics, since they can incorporate large organic dyes [5,6]. Examples of organic dyes that have been incorporated into mesoporous silicates are porphyrins [7], phthalocyanines [8,9], methylene blue [10] and ferrocene [11]. The incorporation of fluorescent dyes is particularly interesting for the construction of optical devices, such as nanolasers and fluorescent nanoparticles for medical diagnosis [12–15], since the organized mesoporous framework usually prevents dye aggregation, increasing the fluorescence. Most studies on the incorporation of fluorescent dyes into mesoporous molecular sieves, however, have been restricted to rhodamine, fluorescein and coumarin derivatives [5,6,12–15]. Our group [16,17] and others [18] have recently reported on the incorporation of a different class of dyes, the 3,4,9,10-perylenediimides (PDI), into the channels of mesoporous materials MCM-41 and SBA-15. In a continuation to our efforts towards preparing new materials based on fluorescent aromatic imides, we report herein on the covalent grafting of 4-amino-1,8-naphthalimides (ANI) in the pores of MCM-41 and SBA-15. A recently published article described the encapsulation of a ANI derivative within the pores of MCM-41 [19], but in that case the dye was incorporated by sorption, and not by covalent bonding.

The 4-amino-1,8-naphthalimides (ANI) constitute a class of strongly fluorescent yellow dyes with very interesting photophysical properties [20–23]. Thank to these properties, the ANI have been used in several applications, ranging from electroluminescent devices [24] to sensors for cations and anions [25–29], molecular switchers [30,31], artificial photosynthetic systems [32–34] and thermochromic [35] and pH sensing [36] devices. The ANI are also useful as building blocks for the construction of supramolecular systems, such as rotaxanes, catenanes [37] and inclusion complexes with cyclodextrins [38,39].

In order to bind covalently the ANI chromophore to MCM-41 and SBA-15, we first modified the pore walls with 3-

* Corresponding author. Tel./fax: +55 11 49963166.
E-mail address: sergio.brochsztain@ufabc.edu.br (S. Brochsztain).

0143-7208/$ – see front matter © 2010 Elsevier Ltd. All rights reserved.
doi:10.1016/j.dyepig.2010.09.009

aminopropyltriethoxysilane (APTES), introducing amino functionalities [40,41] that were further reacted with the precursor molecule 4-amino-1,8-naphthalic anhydride, resulting in ANI-bound mesoporous materials (Scheme 1). The same method was used by our group to obtain PDI grafted MCM-41 and SBA-15 from the reaction of the surface bound amino groups with 3,4,9,10-naphthalenetetracarboxylic dianhydride [17]. Results obtained with a non-porous silica gel modified with ANI by the same method are also presented in this work, as a comparison. Recently, Leng et al. reported the use of a similar method to obtain ANI-grafted MCM-41 for use as a chemosensor for Hg^{2+} cations [42].

2. Experimental section

2.1. Materials

3-Aminopropyltriethoxysilane (APTES) and 4-amino-1,8-naphthalic anhydride were purchased from Aldrich, and used as received. The following HPLC grade solvents were obtained from Baker: chloroform, acetonitrile, toluene, *N*,*N*-dimethylformamide (DMF), ethanol (EtOH) and methanol. Deionized water (Barnstead easypure RF system) was used in all experiments. The mesoporous molecular sieves MCM-41 and SBA-15 were synthesized and characterized as described in our previous reports [16,17]. Silica gel Cab-O-Sil L-90 (supplier data: BET surface area 90 m^2/g, average particle diameter 20 nm) was a gift from Cabot Corporation, and was used as received.

2.2. Instruments

Elemental analysis of the samples were performed at the Chemistry Institute, São Paulo University. Infrared spectra were recorded with the samples in KBr pellets, using a FTIR Perkin-Elmer Spectrum One apparatus. Small angle X-ray scattering (SAXS) experiments were performed in a Rigaku Radiation Shield equipment using a rotating anode and CuK α radiation ($\lambda = 1.5418$ Å), with an image plate detector. The equipment was operated at 10 kW (50 kV and 200 μA), with a distance of 508 mm between the samples and the detector. The samples were placed inside a 1 mm diameter quartz tube and subjected to 2 h of beam exposure. The distance (a_o) between pore centers of the hexagonal structure was calculated with the formula $a_0 = \frac{2d_{(100)}}{\sqrt{3}}$. SEM images were recorded with a Supra 40 scanning electron microscope (Zeiss). Samples were gold coated prior to analysis. Absorption spectra were recorded with a Cary 50 spectrophotometer (Varian). Absorption spectra of the solid samples were taken using the solid sample support of the Cary 50, by pressing the powders in KBr pellets. Fluorescence spectra were registered with a Cary Eclipse fluorescence spectrophotometer (Varian), with the fluorescent powders either placed in a 5 mm NMR tube (for solid state measurements) or suspended in the appropriate solvent in a quartz cuvette (typically 2–3 mg of powder for 3 mL of solvent). After the measurements, the suspensions of the solid materials were filtered through 0.2 μm filters, and the absorption and emission spectra of the filtrates were measured. No detectable ANI absorbance or fluorescence was

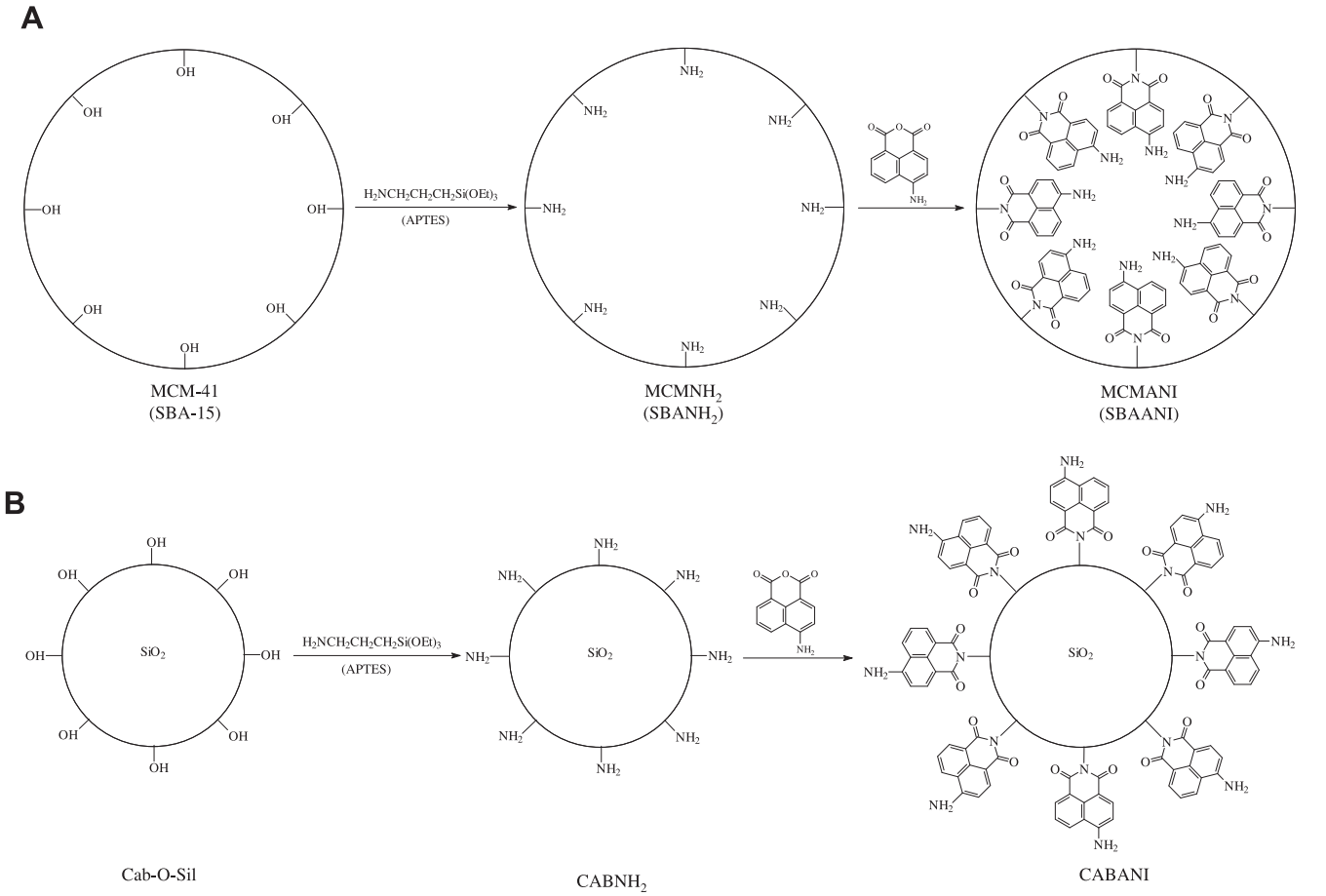

Scheme 1. (A) Modification of mesoporous molecular sieves MCM-41 or SBA-15 with APTES followed by ANI on the inner surface. (B) Modification of non-porous silica gel with APTES followed by ANI on the outer surface.

observed in the filtrates, confirming that the absorption and emission of the suspensions were indeed due to the dye in the solid state, bound to the silicate surface (Scheme 1).

2.3. Methods

Modification of the silica samples with amino groups was carried out by reaction with APTES, according to the previously reported method [17]. Typically, the siliceous material was activated in an oven (110 °C, 20 h) and then allowed to react with APTES in anhydrous toluene for 24 h at 60 °C in a shaker, under an argon atmosphere. The aminated silica was then thoroughly washed, first with toluene, then methanol and finally with water. After each washing step, the silica was separated from the mother liquid by centrifugation (12,000 rpm, 20 min). At the end of the washing steps, the modified samples were dried in an oven (24 h, 120 °C). The amino-modified materials tested positive for ninhydrin (a specific reagent for primary amino groups).

In order to obtain the ANI-grafted samples, the APTES-modified MCM-41 or SBA-15 (50 mg) was suspended in a solution of 4-amino-1,8-naphthalic anhydride (107 mg, 0.5 mmol) in 50 mL of *N*,*N*-dimethylformamide (DMF). The mixture was allowed to react at 120 °C for 30 min, and then washed thoroughly with several portions of hot DMF, followed by ethanol, until the washing solution became colorless, indicating that the excess of the anhydride had been removed. After each washing step, the solid was separated from the mother liquid by centrifugation (12,000 rpm, 20 min). At the end of the washing steps, the remaining yellow powder was dried in an oven (24 h, 120 °C), yielding 46 mg (MCM-41) or 47 mg (SBA-15) of the modified material. For the non-porous silica gel, the same method was employed, using the following amounts: 10.7 mg of 4-amino-1,8-naphthalic anhydride (0.05 mmol) in 50 mL DMF and 110 mg of amino-modified silica gel, giving 109 mg of the yellow powder.

3. Results and discussion

Covalent attachment of the ANI chromophore to the walls of mesoporous molecular sieves, according to Scheme 1, was monitored by several techniques. The elemental analysis of the samples (Table 1) showed a gradual increase in the carbon content after each modification step. After reaction of MCM-41 and SBA-15 with APTES, the percent of C and N rised from trace amounts to *ca* 7% and 2%, respectively, indicating the success of the silanization step. After reaction with 4-amino-1,8-naphthalic anhydride, the C content increased further to *ca* 11%, and the materials, that were initially white, became yellowish and fluorescent under UV irradiation (see Supplementary Material), showing that the chromophore was attached to the silicate surface. The percent of nitrogen actually decreased after reaction with the anhydride, but this result is consistent with the fact that the $-CH_2-CH_2-CH_2-NH_2$ moiety (C/N ratio of 2.58) has a higher percent of N than the fragment $-CH_2-CH_2-CH_2-$ANI (C/N ratio of 6.75).

The non-porous silica, on the other hand, showed a percent of carbon of less than 2% after reaction with APTES, followed by 4-amino-1,8-naphthalic anhydride. These observations suggest that the ANI chromophore was bound to the internal surface of the pores in MCM-41 and SBA-15 (otherwise the amount of organic material would be expectedly similar to the non-porous sample). Similar results were found in our previous work with MCM-41 and SBA-15 modified with the perylenic imide PDI [17].

X-ray diffraction patterns of the samples of MCM-41 and SBA-15 before and after modification with the ANI chromophore are shown in Fig. 1 (a table with the X-ray data is given as Supplementary Material). The peaks corresponding to the reflections (100), (110) and (200), which are characteristic of the hexagonal arrangement found in these mesoporous materials, are clearly seen, even after modification with ANI. These results show that the materials did not lose their mesoporous structures when submitted to the harsh reaction conditions used for grafting the chromophore (Scheme 1), which include treatment with boiling toluene and DMF. The X-ray data also show that the pore size was not changed upon dye

Table 1
Elemental analysis of modified silicate samples.

Material	%C	%N	C/N ratio
MCM-41	0.20	0.03	–
$MCMNH_2$	7.72	2.54	3.04[a]
MCMANI	11.18	2.25	4.97[b]
SBA-15	0.35	0.28	–
$SBANH_2$	6.28	2.29	2.74[a]
SBAANI	11.26	2.23	5.05[b]
Cab-O-Sil	0.23	0.06	–
$CABNH_2$	1.32	0.51	2.59[a]
CABANI	1.81	0.39	4.64[b]

[a] Calculated for $-CH_2CH_2CH_2NH_2 = 2.58$.
[b] Calculated for $-CH_2CH_2CH_2$ANI = 6.75.

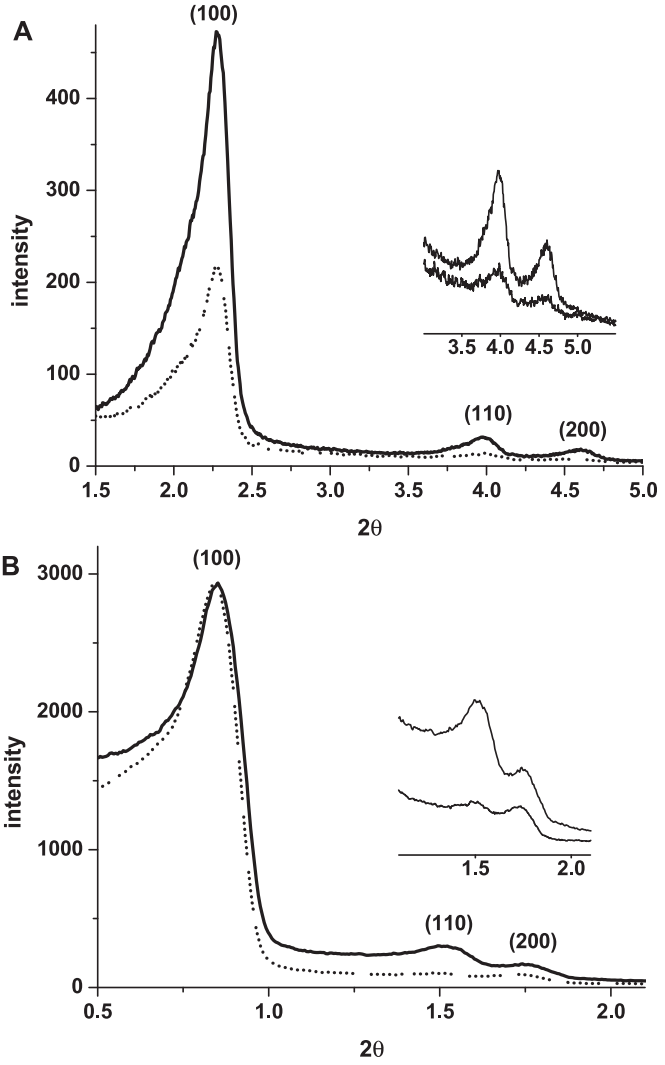

Fig. 1. X-ray diffraction patterns of the modified materials. (A) MCM-41 (solid line) and MCMANI (dotted line). (B) SBA-15 (solid line) and SBAANI (dotted line).

incorporation, since the position of the peaks is the same before and after modification. Note that the peaks in the SBA samples lie at smaller angles than the corresponding peaks in the MCM samples, which is due to the larger pore size of the former, since SBA-type materials are prepared using as templates larger micelles then MCM materials.

The modified materials were also studied by infrared spectroscopy (Fig. 2). The two main absorption bands of ANI derivatives are usually found at *ca* 1700 and 1670 cm^{-1}, corresponding to the asymmetric and symmetric carbonyl stretches, respectively [27,28]. Unfortunately, these imide carbonyl bands in the new materials are masked by the SiO_2 absorption band at 1637 cm^{-1}. However, it is still possible to identify some features that are characteristic of the organic modifier (Fig. 2), such as the C–H stretching bands (2900–2950 cm^{-1}), which are due to the propyl linker, and the band due to the aromatic C=C stretch (Fig. 2), which appears at 1552 cm^{-1} (MCMANI) and 1562 cm^{-1} (SBAANI). Another band at 1379 cm^{-1}, which is also characteristic of ANI derivatives, can be seen in the spectrum of SBAANI.

The modified mesoporous samples were also studied by scanning electron microscopy (SEM). The general morphology of the particles was not altered by the modification reactions employed (Fig. 3). In the case of SBA-15, the material consisted of 20–30 μm long bundles of parallel or intertwinned fibrils with diameter ranging from 0.5–1 μm (Fig. 3A). The general aspect of the material remained the same after the modification reactions (Fig. 3B and C). The presence of the mesoporous channels in SBAANI could be clearly visualized in high magnification SEM images (Fig. 3C), confirming that the mesoporous structure of the materials was retained during the treatment used for the modification with the dye (Scheme 1). In the case of MCM-41, the particles had a less defined shape than in the case of SBA-15, and the mesoporous channels could not be seen clearly in the images (see Supplementary Material).

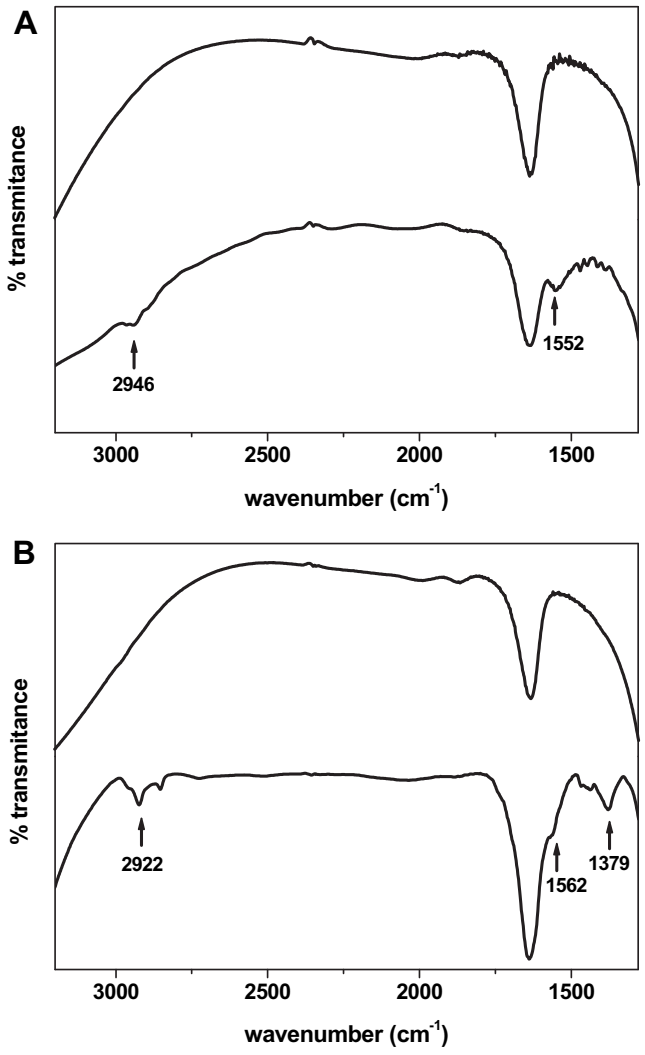

Fig. 2. Infrared spectra of modified and non-modified mesoporous materials: (a) non-modified MCM-41 (top) and MCMANI (bottom). (b) Non-modified SBA-15 (top) and SBAANI (bottom).

The ANI-modified materials were also studied by absorption and emission spectroscopy, as shown in Figs. 4–7. Fig. 4A shows the absorption spectra of the solid samples pressed in KBr pellets. The spectra were normalized for the sake of comparison. A quantitative analysis using Lambert-Beer's law was not possible, since the dye concentration in the KBr pellets was too high and the spectra had to be baseline corrected due to scattering by the silica. The samples CABANI and MCMANI showed the same absorption maxima at 438 nm, whereas SBAANI absorption peaked at 423 nm. These maxima can be compared with those for *N*-carboethoxy-4-amino-1,8-naphthalimide (ANIGLI), a representative ANI derivative, in solution. The absorption maxima for this compound was red-shifted from 408 nm in chloroform to 430 nm in ethanol, suggesting that the ANI molecules feel a high polarity environment in the solid samples. These results, however, can be attributed to the presence of KBr, since the samples had to be dispersed in an optically transparent matrix for the absorption measurements. The fluorescence data, on the other hand, were collected with the solid materials without any treatment, and therefore give more reliable structural information.

The normalized emission spectra of the solid samples are shown in Fig. 4B (emission maxima are summarized in Table 2). The ANI chromophore bound to the external surface of CABANI showed emission maximum at 518 nm, in contrast to the dye bound to the inner pore walls, as in MCMANI and SBAANI, where the emission maxima were red-shifted to 533 nm. These results suggest that the ANI chromophore confined within the mesopores feels a polar microenvironment due to the presence of surface hydroxyl groups.

Furthermore, dye fluorescence in the MCMANI and SBAANI samples was highly quenched as compared to that in CABANI. Quantum yield measurements are very difficult to perform in the solid state, since the emission intensity depends, among other factors, on the geometry of the solids. However, the emission of the dye in CABANI was several orders of magnitude more intense than that observed in the case of the mesoporous samples (note that the spectra in Fig. 4B were normalized for comparison). The emission of MCMANI and SBAANI was very weak, and could be detected only by using the highest detector sensitivity, whereas in the case of CABANI the lowest sensitivity had to be used to avoid optical saturation of the photomultiplier tube. The observed fluorescence quenching suggests that the ANI molecules were stacked within the mesopores of MCM-41 and SBA-15, in contrast to the externally bound ANI molecules in the non-porous silica. Chen et al. have also observed fluorescence quenching for a ANI derivative incorporated by sorption into the pores of MCM-41 [19]. The behavior of the ANI-modified materials was in striking contrast to the case of the PDI dyes, whose fluorescence was turned on inside the mesoporous channels [17]. A possible explanation for the different behavior could arise from the fact that PDI is a bisimide, and therefore it was attached by both ends to the pore walls, thus decreasing the freedom of motion and the vibrational decay of the excited states.

The fluorescence of the ANI-modified materials was further recorded with the solids dispersed in different solvents, in order to

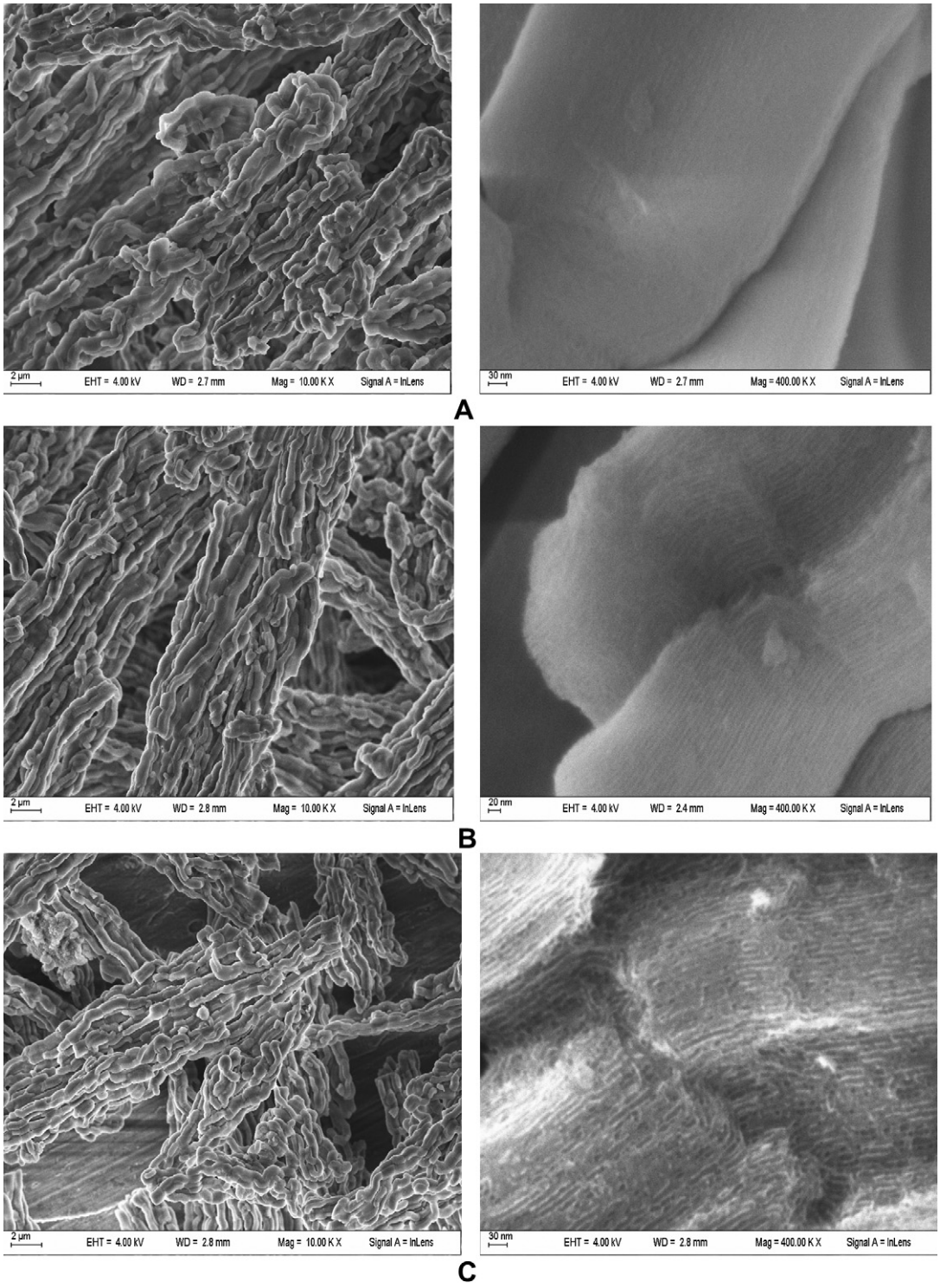

Fig. 3. Scanning electron microscopy images of SBA-15 before and after modification with APTES and ANI. Images at the left side were taken with a magnification of 1,000 X. Images at the right side were taken with a magnification of 40,000 X. (A) Non-modified SBA-15. (B) SBA-15 modified with APTES ($SBANH_2$). (C) SBA-15 modified with APTES, followed by ANI (SBAANI).

study the solvation of the dye molecules in the materials. The results are compared in Table 2 with the data obtained for ANIGLI in solution. It can be noticed that the emission maxima of ANIGLI in solution were quite sensitive to solvent polarity, with an observed red shift of nearly 40 nm when going from an apolar ($\lambda_{max}^{em} = 501$ nm in chloroform) to a polar solvent ($\lambda_{max}^{em} = 540$ nm in water). The pronounced solvent sensitivity observed in the optical spectra of ANI derivatives is well-known [32,33], and has been attributed to the charge-transfer character of the $S_0 \rightarrow S_1$ and $S_1 \rightarrow S_0$ transitions. The excited state of the ANI chromophore is fully charge-separated, displaying a dipole moment in the order of 12 D [33], which is a very high value for organic compounds.

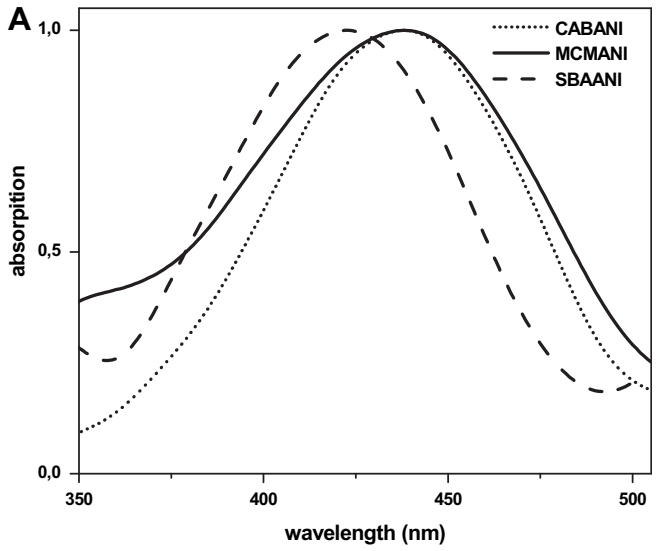

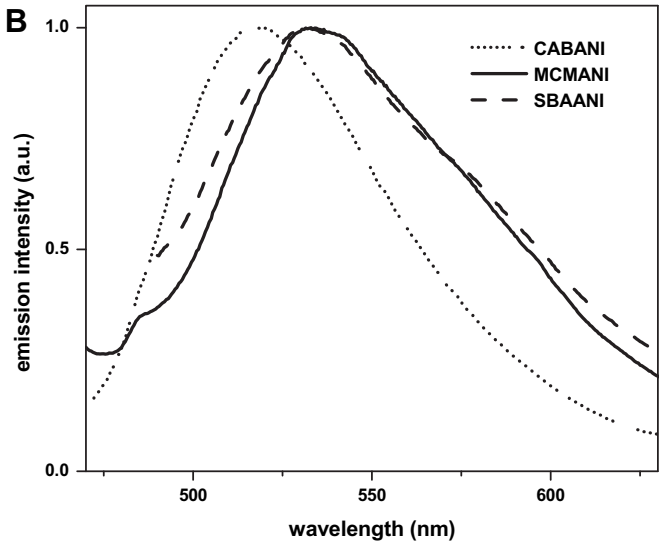

Fig. 4. (A) Solid-state absorption spectra of the ANI-modified materials dispersed in KBr pellets. (B) Normalized solid-state emission spectra of the ANI-modified materials (excitation: 430 nm).

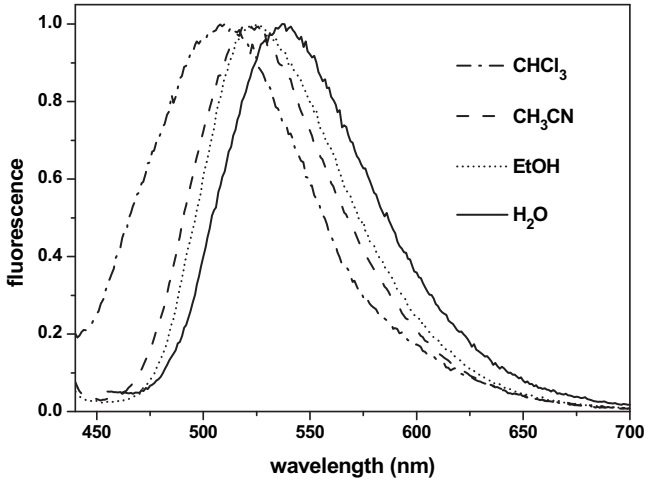

Fig. 5. Normalized emission spectra of CABANI suspensions in solvents of different polarities. Excitation: 430 nm.

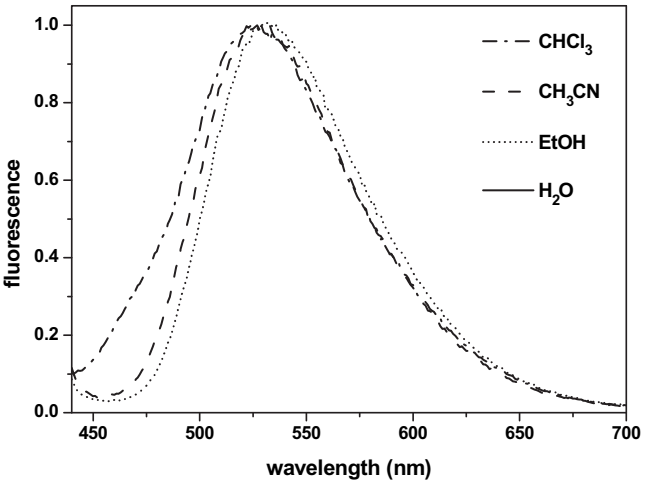

Fig. 6. Normalized emission spectra of MCMANI suspensions in solvents of different polarities. Excitation: 430 nm.

Fig. 5 shows that the solvent effects on the CABANI sample are similar to those observed with ANIGLI in solution, indicating that the externally bound chromomophore (Scheme 1) was exposed to the environment, and therefore well solvated. Emission maxima of CABANI range from 510 to 537 nm as going from chloform to water (Table 2). However, when the same experiment was performed with MCMANI (Fig. 6), a very low solvent sensitivity was observed, with the emission maxima shifting from 527 nm in chloform to 534 nm in water. The striking different behavior of MCMANI suggests that the dye molecules fit tightly within the channels of MCM-41, leaving no room for the solvent molecules to enter. Therefore, the dye molecules are poorly solvated in MCMANI (they rather feel the hydroxyl rich microenvironment provided by the inner pore walls). In the case of SBAANI, solvent sensitivity was restored (Fig. 7), with an observed red-shift of 518 nm in chloform to 535 nm in water. This can be explained by the much larger pore size of SBA-15, leaving enough space for the solvent molecules to invade the channels and partly solvate the ANI molecules.

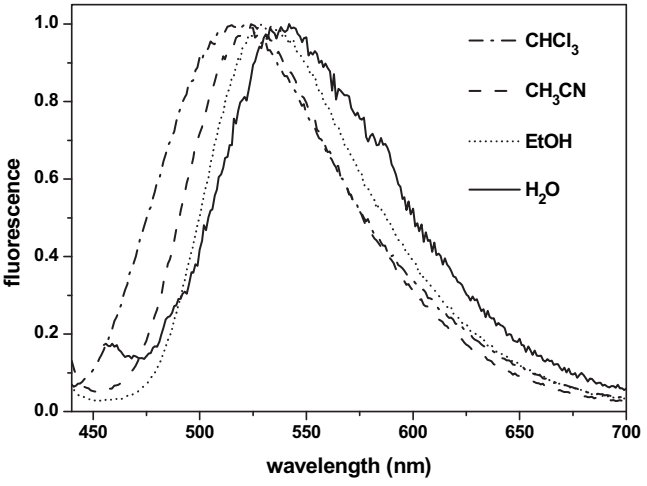

Fig. 7. Normalized emission spectra of SBAANI suspensions in solvents of different polarities. Excitation: 430 nm.

Table 2
Emission maxima (nm) for the ANI-modified mesoporous materials in the solid state or suspended in different solvents. Data for ANIGLI (a representative ANI derivative) in solution are included for comparison.

solvent	CABANI	MCMANI	SBAANI	ANIGLI[a]
$CHCl_3$	510	527	518	501
CH_3CN	522	530	524	508
EtOH	525	531	530	517
H_2O	537	534	535	540
solid state	518	533	533	–

[a] *N*-carboethoxy-4-amino-1,8-naphthalimide (ANIGLI).

4. Conclusions

The present work has shown the general applicability of the method developed by our group towards the covalent grafting of aromatic imides, such as the ANI and PDI, to the inner surface of mesoporous molecular sieves, by reacting the precursors aromatic anhydrides with amino-modified surfaces. X-ray analysis and SEM images showed that the mesoporous structures were preserved during the modification reactions, in spite of the harsh conditions employed, which include reflux in DMF, a high boiling solvent. The different solvent sensitivity observed for dye emission in the different materials has potential applications as size exclusion sensors for solvents.

Acknowledgments

This work was supported by grants from Brazilian agency FAPESP (grant Nº 05/51104-4 and 08/57940-7). S. B. thanks CNPq for a PQ scholarship. F. J. T. is grateful to FAPESP for a doctoral fellowship. The authors thank Prof. Marcia C. A. Fantini, responsible for the Crystallography Laboratory at São Paulo University, for allowing the use of the SAXS equipment. Cabot Corporation is greatly acknowledged for the gift of a sample of Cab-O-Sil L-90.

Appendix. Supplementary data

Supplementary data associated with this article can be found in the online version, at doi:10.1016/j.dyepig.2010.09.009.

References

[1] Kresge CT, Leonowicz ME, Roth WJ, Vartuli JC, Beck JS. Ordered mesoporous molecular sieves synthesized by a liquid-crystal template mechanism. Nature 1992;359:710–2.
[2] Zhao D, Feng J, Huo Q, Melosh N, Fredrickson GH, Chmelka BF, et al. Triblock copolymer syntheses of mesoporous silica with periodic 50 to 300 angstrom pores. Science 1998;279:548–52.
[3] Morin S, Ayrault P, El-Mouahid S, Gnep NS, Guisnet M. Particular selectivity of m-xylene isomerization over MCM-41 mesoporous aluminosilicates. Applied Catalysis A: General 1997;159:317–31.
[4] Seddegi ZS, Budrthumal U, Al-Arfaj AA, Al-Amer AM, Barri SAI. Catalytic cracking of polyethylene over all-silica MCM-41 molecular sieve. Applied Catalysis A: General 2002;225:167–76.
[5] Schulz-Ekloff G, Wöhrle D, vanDuffel B, Schoonheydt RA. Chromophores in porous silicas and minerals: preparation and optical properties. Microporous and Mesoporous Materials 2002;51:91–138.
[6] Brühwiler D, Calzaferri G. Molecular sieves as host materials for supramolecular organization. Microporous and Mesoporous Materials 2004;72:1–23.
[7] Tanaka H, Usui T, Sugiyama S, Horibe S, Shiratori H, Hino R. Incorporation of porphyrins into mesopores of MCM-41. Journal of Colloid and Interface Science 2005;291:465–70.
[8] Tanamura Y, Uchida T, Teramae N, Kikuchi M, Kusaba K, Onodera Y. Ship-in-a-bottle synthesis of copper phthalocyanine molecules within mesoporous channels of MCM-41 by a chemical vapor deposition method. Nano Letters 2001;1:387–90.
[9] Ganschow M, Wöhrle D, Schulz-Ekloff G. Incorporation of differently substituted phthalocyanines into the mesoporous molecular sieve Si-MCM-41. Journal of Porphyrins and Phthalocyanines 1999;3:299–309.
[10] Boboardo S, Borello L, Fiorilli S, Garrone E, Onida B, Arean CO, et al. Methylene blue encapsulated in silica-based mesophases: characterisation and electrochemical activity. Microporous and Mesoporous Materials 2005;79:275–81.
[11] Rohlfing DF, Rathousky J, Rohlfing Y, Bartels O, Wark M. Functionalized mesoporous silica films as a matrix for anchoring electrochemically active guests. Langmuir 2005;21:11320–9.
[12] Ganschow M, Wark M, Wöhrle D, Schulz-Ekloff G. Anchoring of functional dye molecules in MCM-41 by microwave-assisted hydrothermal cocondensation. Angewandte Chemie International Edition 2000;39:160–3.
[13] Zhao W, Li D, He B, Zhang J, Huang J, Zhang L. The photoluminescence of coumarin derivative encapsulated in MCM-41 and Ti-MCM-41. Dyes and Pigments 2005;64:265–70.
[14] Yang P, Wirnsberger G, Huang HC, Cordero SR, McGehee MD, Scott B, et al. Mirrorless lasing from mesostructured waveguides patterned by soft lithography. Science 2000;287:465–7.
[15] Sokolov I, Kievsky YY, Kaszpurenko JM. Self-assembly of ultrabright fluorescent silica particles. Small 2007;3:419–23.
[16] Castro FL, Santos JG, Fernandes GJT, Araújo AS, Fernandes Jr VJ, Politi MJ, et al. Solid state fluorescence of a 3,4,9,10-perylenetetracarboxylic diimide derivative encapsulated in the pores of mesoporous silica MCM-41. Microporous and Mesoporous Materials 2007;102:258–64.
[17] Trindade FJ, Fernandes GJT, Araújo AS, Fernandes Jr VJ, Silva BPG, Nagayasu RY, et al. Covalent attachment of 3,4,9,10-perylenediimides onto the walls of mesoporous molecular sieves MCM-41 and SBA-15. Microporous and Mesoporous Materials 2008;113:463–71.
[18] Wahab MA, Hussain H, He C. Photoactive perylenediimide-bridged silsesquioxane functionalized periodic mesoporous organosilica thin films (PMO-SBA15): synthesis, self-assembly, and photoluminescent and enhanced mechanical properties. Langmuir 2009;25:4743–50.
[19] Chen G, Wang L, Zhang J, Chen F, Anpo M. Photophysical properties of a naphthalimide derivative encapsulated within Si-MCM-41, Ce-MCM-41 and Al-MCM-41. Dyes and Pigments 2009;81:119–23.
[20] Alexiou MS, Tychopoulos V, Ghorbanian S, Tyman JHP, Brown RG, Brittain PI. The UV–visible absorption and fluorescence of some substituted 1,8-naphthalimides and naphthalic anhydrides. Journal of the Chemical Society, Perkin Transactions 1990;2:837–42.
[21] Saha S, Samanta A. Influence of the structure of the amino group and polarity of the medium on the photophysical behavior of 4-amino-1,8-naphthalimide derivatives. Journal of Physical Chemistry A 2002;106:4763–71.
[22] Qian J, Xu Y, Qian X, Wang J, Zhang S. Effects of anionic surfactant SDS on the photophysical properties of two fluorescent molecular sensors. Journal of Photochemistry and Photobiology A: Chemistry 2008;200:402–9.
[23] Loving G, Imperiali B. A versatile amino acid analogue of the solvatochromic fluorophore 4-*N*, *N*-dimethylamino-1,8-naphthalimide: a powerful tool for the study of dynamic protein interactions. Journal of the American Chemical Society 2008;130:13630–8.
[24] Morgado J, Gruner J, Walcott SP, Yong TM, Cervini R, Moratti SC, et al. 4-AcNI—a new polymer for light-emitting diodes. Synthetic Metals 1998; 95:113–7.
[25] Mitchell KA, Brown RG, Yuan D, Chang SC, Utecht RE, Lewis DE. A fluorescent sensor for Cu2+ at the sub-ppm level. Journal of Photochemistry and Photobiology A: Chemistry 1998;115:157–61.
[26] Veale EB, Gunnlaugsson T. Bidirectional Photoinduced Electron-Transfer Quenching Is Observed in 4-Amino-1,8-naphthalimide-Based Fluorescent Anion Sensors. Journal of Organic Chemistry 2008;73:8073–6.
[27] Bojinov VB, Georgiev NI, Bosch P. Design and synthesis of highly photostable yellow–green emitting 1,8-naphthalimides as fluorescent sensors for metal cations and protons. Journal of Fluorescence 2009;19:127–39.
[28] Bojinov VB, Panova IP, Chovelon JM. Novel blue emitting tetra- and pentamethylpiperidin-4-yloxy-1,8-naphthalimides as photoinduced electron transfer based sensors for transition metal ions and protons. Sensors and Actuators B: Chemical 2008;135:172–80.
[29] Leng B, Zou L, Jiang J, Tian H. Colorimetric detection of mercuric ion (Hg^{2+}) in aqueous media using chemodosimeter-functionalized gold nanoparticles. Sensors and Actuators B: Chemical 2009;140:162–9.
[30] Poteau X, Brown AI, Brown RG, Holmes C, Matthew D. Fluorescence switching in 4-amino-1,8-naphthalimides: "on–off–on" operation controlled by solvent and cations. Dyes and Pigments 2000;47:91–105.
[31] Ferreira R, Remon P, Pischel U. Multivalued Logic with a Tristable Fluorescent Switch. Journal of Physical Chemistry C 2009;113:5805–11.
[32] Greenfield SR, Svec WA, Gosztola D, Wasielewski MR. Multistep Photochemical Charge Separation in Rod-like Molecules Based on Aromatic Imides and Diimides. Journal of the American Chemical Society 1996;118:6767–77.
[33] Silva AP, Rice TE. A small supramolecular system which emulates the unidirectional, path-selective photoinduced electron transfer (PET) of the bacterial photosynthetic reaction centre (PRC). Chemical Communications; 1999: 163–4.
[34] Georgiev NI, Bojinov VB. The design and synthesis of a novel 1,8-naphthalimide PAMAM light-harvesting dendron with fluorescence "off-on" switching core. Dyes and Pigments 2010;84:249–56.
[35] Li C, Du P, Tian H, Erk P. Novel thermochromic copolymers with two luminescent colors. Chemistry Letters 2003;32:570–1.
[36] Niu CG, Zeng GM, Chen LX, Shen GL, Yu RQ. Proton off-on behaviour of methylpiperazinyl derivative of naphthalimide: a pH sensor based on fluorescence enhancement. Analyst 2004;129:20–4.

[37] Qu DH, Wang QC, Tian H. A half adder based on a photochemically driven [2]rotaxane. Angewandte Chemie International Edition 2005;44:5296–9.
[38] Campos IB, Brochsztain S. Inclusion complexes of cyclodextrins with 4-amino-1,8-naphthalimides. Journal of Inclusion Phenomena and Macrocyclic Chemistry 2002;44:207–11.
[39] Silva BG, Marcon RO, Brochsztain S. Inclusion complexes of cyclodextrins with 4-amino-1,8-naphthalimides (part 2). Journal of Inclusion Phenomena and Macrocyclic Chemistry; 07 May 2010; doi:10.1007/s10847-010-9790-8. published online.
[40] Shephard DS, Zhou W, Maschmeyer T, Matters JM, Roper CL, Parsons S, et al. Site-directed surface derivatization of MCM-41: use of high-resolution transmission electron microscopy and molecular recognition for determining the position of functionality within mesoporous materials. Angewandte Chemie International Edition 1998;37:2719–23.
[41] Chong ASM, Zhao XS. Functionalization of SBA-15 with APTES and characterization of functionalized materials. Journal of Physical Chemistry B 2003;107:12650–7.
[42] Leng B, Jiang J, Tian H. A mesoporous silica supported Hg^{2+} chemodosimeter. AIChE Journal 2010;56:2957–64.